Supporting information for: Ion Fluctuations and Intermembrane Interactions in Aqueous Dispersions of Dialkylchain Cationic Surfactant Studied by Dielectric Relaxation Spectroscopy and Small- and Wide-Angle X-ray Scattering

Keiichi Yanase,[a] Miku Obikane,[a] Taku Ogura,*[b] Richard Buchner,[c]
Akinori Igarashi,[b] and Takaaki Sato*[a]

[a]Department of Chemistry and Materials, Faculty of Textile Science and Technology,
Shinshu University, Ueda, Nagano 386-8567, Japan.
[b]Research & Development Headquarters, LION Corporation,
Tokyo 132-0035, Japan.
[c]Institut für Physikalische und Theoretische Chemie, Universität Regensburg,
93040 Regensburg, Germany.

*E-mail: takaakis@shinshu-u.ac.jp (T.S.), t-ogura@lion.co.jp (T.O.)

Contents

- Density and viscosity data.
- Simulated relaxation amplitudes of ion fluctuation processes based on the Grosse theory.
- Interaction potential calculations based on the DLVO theory, Sogami-Ise theory, and the modified DLVO theory of Hishida.
- SAXS experiments performed with a pinhole camera.
- Microscope observations.

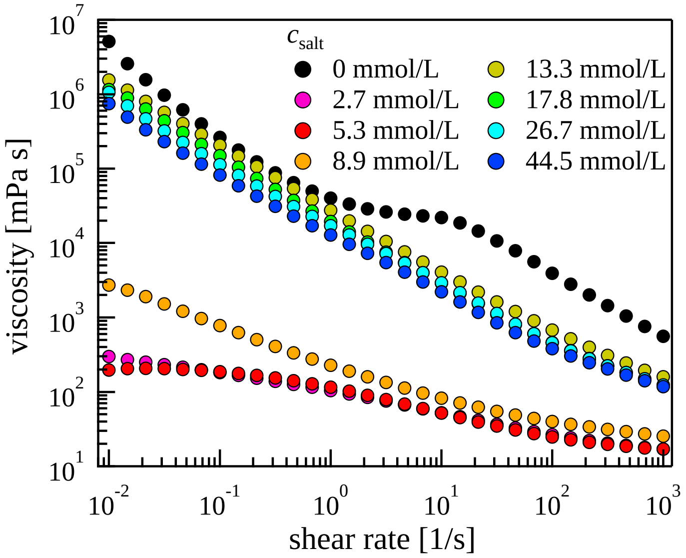

Figure S1: Viscosities of 2HT dispersions at different $CaCl_2$ concentrations at 25 °C as a function of the share rate.

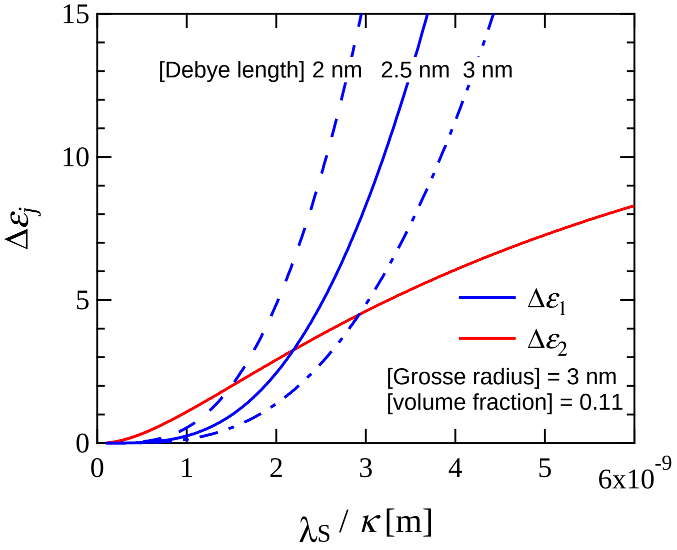

Figure S2: Simulated relaxation amplitudes of the ion-cloud fluctuation, $\Delta\varepsilon_1$ (eq. 4), and the surface-hopping mode, $\Delta\varepsilon_2$ (eq. 6), as a function of the relative surface conductivity against the bulk conductivity, $\lambda_{\mathrm{S}}/\kappa$. The Grosse radius and the volume fraction are fixed to 3 nm and 0.11, respectively. The simulated $\Delta\varepsilon_1$ with the Debye length of 2 nm, 2.5 nm, and 3 nm are represented by the blue dashed, solid, and dash-dot lines, respectively.

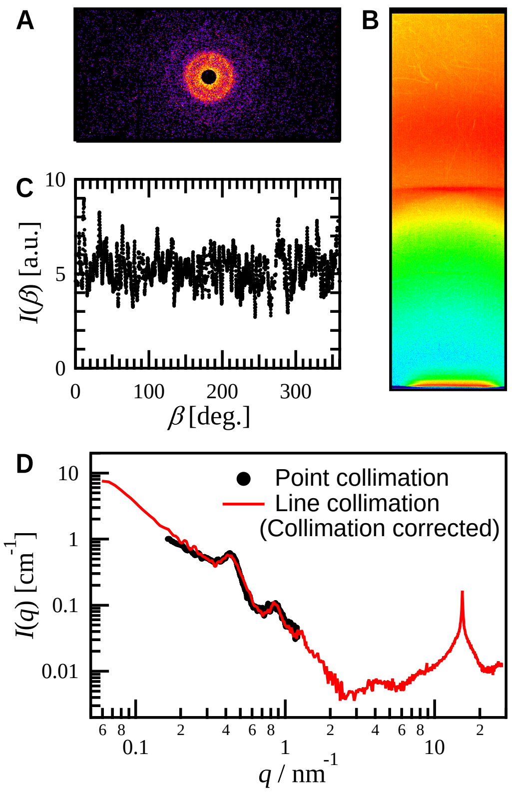

Figure S3: Two-dimensional scattering patterns of the 2HT dispersion at $CaCl_2$ concentration of 2.7 mmol/L as obtained by (A) a point collimation SmartLab apparatus and (B) a line collimation SAXSess mc^2 apparatus. One-dimensional scattering intensities as a function of (C) the magnitude of the azimuthal angle, β, and (D) the scattering vector, q, respectively. The azimuthal profile, $I(\beta)$, is obtained by integrating the point collimated $I(q)$ in the q-range between 0.36 and 0.48 nm^{-1}, corresponding to the scattering angles of $0.51°$ and $0.67°$. For $I(q)$ data measured by the line collimation apparatus, a desmearing procedure is made by relying on the Lake algorithm[S1]. The background contribution and transmission calibration are corrected. It is well established that liquid-like systems, e.g., α-gels, lamellar lyotropic liquid crystals[S2] and multi-lamellar vesicles[S3,S4] exhibit isotropic scattering patterns under static condition. Furthermore, the isotropic diffraction ring has been taken as evidence of the lamellar-to-onion (MLV) transition under an applied shear. We confirm that the 2HT dispersion exhibits isotropic scattering patterns and the collimation-corrected $I(q)$ measured by the line-collimation apparatus well coincide with that measured by the point collimated apparatus.

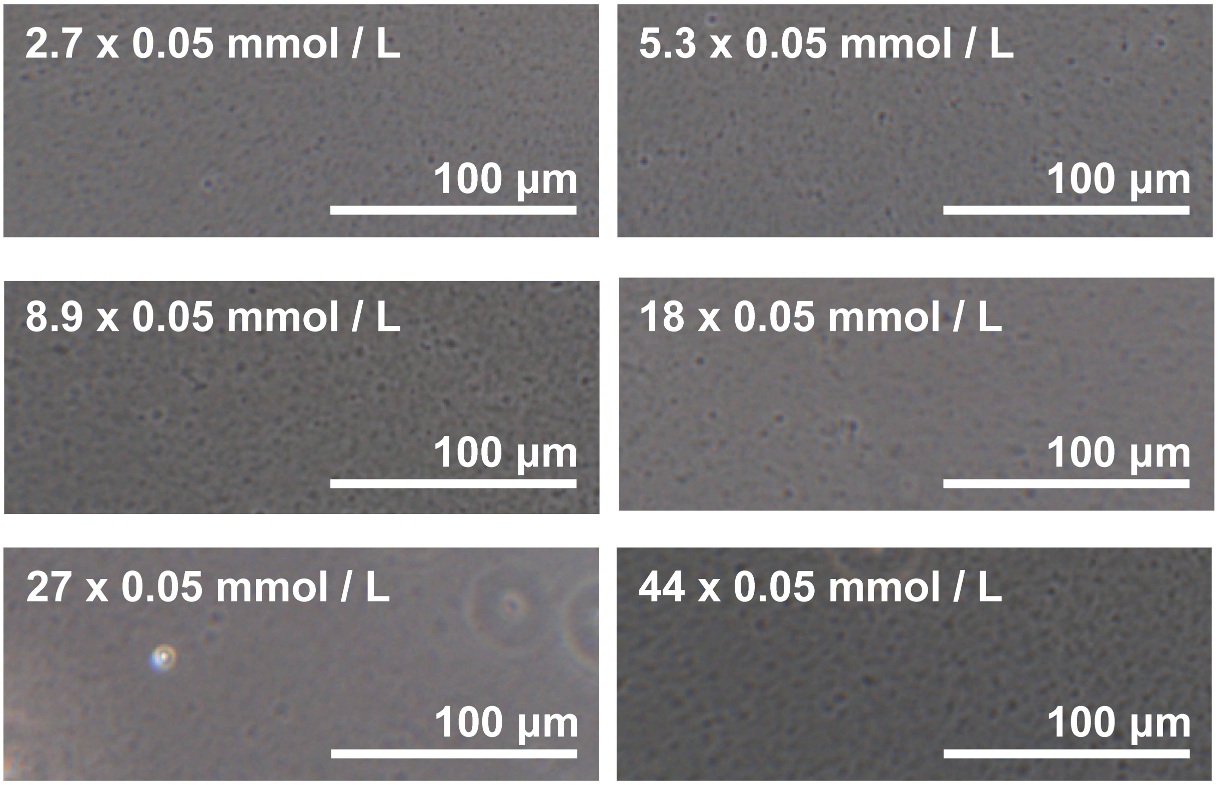

Figure S4: Phase-contrast micrographs of diluted 2HT dispersions (scale bar = 100 µm). These dispersions were prepared by diluting the mother dispersions of 2HT at different $CaCl_2$ salt concentrations by 20 times with Millipore water.

Interactions between the 2HT membranes.

To model interactions between the 2HT membranes, we calculated interaction free energy for two flat surfaces per unit area based on Derjaguin-Landau-Verwey-Overbeek (DLVO) theory, accounting for the attractive van der Waals and repulsive electric double-layer forces[S5–S8]. The total potential, $V_{\rm DLVO}$, between the surfaces can be described as the sum of two contributions, the van der Waals interaction, $V_{\rm A}$, and the electric double-layer interaction, $V_{\rm R}$ as $V_{\rm DLVO} = V_{\rm A} + V_{\rm R}$, where

$$V_{\rm A} = -\frac{A}{12\pi}\left\{\frac{1}{h^2} + \frac{1}{(h+2\delta)^2} - \frac{2}{(h+\delta)^2}\right\} \tag{S1}$$

and

$$V_{\rm R} = 64nk_{\rm B}T\chi^{-1}\left[\tanh(\frac{e\psi_0}{4k_{\rm B}T})\right]^2 \exp(-\chi h). \tag{S2}$$

A, h, δ, n, e and ψ_0 respectively denote the Hamaker constant, surface separation, the bilayer thickness, number density of ions, charge of an electron, and surface potential obtained from the equation, $\sigma_0 = (8N_{\rm A}I\varepsilon_0\varepsilon_{\rm m}k_{\rm B}T)^{1/2}\sinh(\frac{e\psi_0}{2k_{\rm B}T})$, where σ_0 is the surface charge density and I is the ionic strength. The van der Waals potential between two flat surfaces, $V_{\rm A}$, has a distance dependence of $V_{\rm A} \sim h^{-2}$ as indicated by eq. S1, thereby being inherently short-ranged and causing strong adhesion at a contact distance. The strength and the screening of the electrostatic double-layer potential are mainly determined by the surface charge density and the salinity of the intervening water, respectively. Higher salt concentration results in the faster decay of the potential. Monolayer compression isotherms of dialkyl dimethyl ammonium salt surfactants indicated the headgroup area of ca. 60 Å^2, whereas ca. 40 Å^2 is obtained if all hydrocarbon chains are assumed to be crystalline and packed into a hexagonal lattice having a repeat distance of 4.2 Å.

We also tested Sogami-Ise potential, $V_{\rm SI}$, which assumes a weak long-range electrostatic attraction mediated by the intermediate counterions,[S9–S12]

$$V_{\mathrm{SI}} = \frac{{\sigma_0}^2}{\varepsilon_{\mathrm{m}}\varepsilon_0}\frac{\exp(-\chi h)}{\chi}(3-\chi h). \qquad \text{(S3)}$$

The depth of the potential minimum becomes shallower at higher salt concentration, where the surfaceseparation is smaller.

Recently, Hishida and coworkers suggested the modified electric double layer interaction potential, V_{DL}, given by

$$V_{\mathrm{DL}} = \frac{2\pi\varepsilon_{\mathrm{m}}\varepsilon_0 \left(k_{\mathrm{B}}T\right)^2}{e^2}\left(\frac{1}{h}-\frac{1}{h_{\max}}\right)+\frac{2I-\rho_0}{Z}k_{\mathrm{B}}TN_{\mathrm{A}}\left(h-h_{\max}\right), \qquad \text{(S4)}$$

in which additional osmotic pressure arising from an ion concentration difference between inner and outer aqueous phases separated by vesicle architecture is taken into account[S13]. The modified DLVO potential, $V_{\mathrm{mod-DLVO}}$, is thus given by a sum of the van der Waals and the modified electric double layer potentials as $V_{\mathrm{mod-DLVO}} = V_{\mathrm{A}} + V_{\mathrm{DL}}$. They claimed that this model can explain co-ion-valence effects on the lamellar repeat distance between anionic bilayers. Within the framework of this model, the potential minimum becomes markedly deeper with increasing salt concentration, which predicts a highly ordered state of the membranes at higher salt concentration.

The interaction free energies, V_{DLVO}, V_{SI}, and $V_{\mathrm{mod-DLVO}}$, are shown in Figure 9 and all parameters used in this calculation are listed in Tables S2, S3, and S4.

Table S1: Densities of the dispersions. The 2HT concertation was fixed to 10 wt.%, corresponding to 0.174 mol/L.

$CaCl_2$ concentration [mmol/L]	density [g/cm^3]
0	0.987^F
2.7	0.98617
5.3	0.98711
8.9	0.98701
13.3	0.987^F
17.8	0.987^F
26.7	0.987^F
44.5	0.987^F

^{F} Fixed value

Table S2: Parameters used for calculating DLVO interaction free energy, V_{DLVO}, for two charged flat surfaces shown in Figure 9A.

Parameter	value
Boltzmann constant k_{B} [J/K]	1.38×10^{-23}
permittivity of vacuume ε_0 [C/V m]	8.85×10^{-12}
Avogadro number N_{A} [mol^{-1}]	6.02×10^{23}
charge of an electron e [C]	1.60×10^{-19}
(relative) permittivity of solvent ε_{m} [-]	78.36
Temperature T [K]	298.15
Hamaker constant A [J]	5×10^{-21}
surface charge density σ_0 [C/m^2]	4.0×10^{-2}
layer thickness δ [nm]	4.8
degree of counterion dissociation [-]	0.1

Table S3: Parameters used for calculating effective potential of Sogami-Ise, V_{SI}, for two charged flat surfaces shown in Figure 9B.

Parameter	value
Boltzmann constant k_{B} [J/K]	1.38×10^{-23}
permittivity of vacuume ε_0 [C/V m]	8.85×10^{-12}
Avogadro number N_{A} [mol^{-1}]	6.02×10^{23}
charge of an electron e [C]	1.60×10^{-19}
(relative) permittivity of solvent ε_{m} [-]	78.36
Temperature T [K]	298.15
surface charge density σ_0 [C/m^2]	4.0×10^{-2}

Table S4: Parameters used for calculating modified DLVO interaction free energy, $V_{\mathrm{mod-DLVO}}$, shown in Figure 9C.

Parameter	value
Boltzmann constant k_{B} [J/K]	1.38×10^{-23}
permittivity of vacuume ε_0 [C/V m]	8.85×10^{-12}
Avogadro number N_{A} [mol^{-1}]	6.02×10^{23}
charge of an electron e [C]	1.60×10^{-19}
(relative) permittivity of solvent ε_{m} [-]	78.36
Temperature T [K]	298.15
Hamaker constant A [J]	5×10^{-21}
layer thickness δ [nm]	4.8
concentration of the counter ion originally stuck to 2HT ρ_0 [mol/cm^3]	1.74×10^{-5}
valence of the ionic species Z [-]	2
maximum surface separation $h_{\max}$ [nm]	38.8
degree of counterion dissociation [-]	0.1

References

(S1) J. Lake, *Acta Crystallogr.*, 1967, **23**, 191–194.

(S2) A. S. Poulos, M. Nania, P. Lapham, R. M. Miller, A. J. Smith, H. Tantawy, J. Caragay, J. Gummel, O. Ces, E. S. J. Robles and J. T. Cabral, *Langmuir*, 2016, **32**, 5852–5861.

(S3) A. Bóta, Z. Varga and G. Goerigk, *J. Phys. Chem. B Lett.*, 2007, **111**, 1911–1915.

(S4) A. Bóta, Z. Varga and G. Goerigk, *J. Appl. Crystallogr.*, 2007, **40**, s259–s263.

(S5) B. Derjaguin and L. Landau, *Acta Physicochim. URSS*, 1941, **14**, 633–662.

(S6) E. J. W. Verwey and J. T. G. Overbeek, *Theory of the stability of lyophobic colloids*, Elsevier, 1948.

(S7) J. N. Israelachvili and P. M. McGuiggan, *Science*, 1988, **241**, 795–800.

(S8) J. N. Israelachvili, *Intermolecular and surface forces*, Academic Press, 3rd edn., 2011.

(S9) I. Sogami, *Phys. Lett. A*, 1983, **96**, 199–203.

(S10) I. Sogami and N. Ise, *J. Chem. Phys.*, 1984, **81**, 6320–6332.

(S11) M. Smalley, *Mol. Phys.*, 1990, **71**, 1251–1267.

(S12) F. Geng, R. Ma, A. Nakamura, K. Akatsuka, Y. Ebina, Y. Yamauchi, N. Miyamoto, Y. Tateyama and T. Sasaki, *Nat. Commun.*, 2013, **4**, 1632.

(S13) M. Hishida, Y. Nomura, R. Akiyama, Y. Yamamura and K. Saito, *Phys. Rev. E*, 2017, **96**, 040601.